JOURNAL OF MATERIALS SCIENCE 17 (1982) 1571–1578

Evaluation of the microstructure of ß-SiAlON solid solution materials containing different amounts of amorphous grain boundary phase

P. GREIL, J. WEISS
Max-Planck-Institut für Metallforschung, Institut für Werkstoffwissenschaften, Stuttgart, W. Germany

In order to test the possibility of quantitative microstructural anlaysis in Si_3N_4 ceramics, β solid solution materials containing different amounts of an amorphous phase were examined by transmission electron microscopy. The results show the amount and distribution of the amorphous phase and the influence of this phase on the grain morphology. This shows that within certain limits, set by the transmission electron microscopy, such a characterization is possible.

1. Introduction

Recent investigations in Si_3N_4 ceramics using transmission electron microscopy (TEM) show the presence of small fractions of an amorphous phase present between grain boundaries and in triple-points [1–9]. This oxygen-rich silicate-type phase yields a strength degradation at high temperatures by a grain boundary sliding mechanism [10–13]. The factors responsible for its formation are:

(i) The densification of Si_3N_4 ceramics in general is produced by a transient liquid phase [14, 15] which crystallizes incompletely upon cooling. This too applies for SiAlON materials [16, 17] and is of special importance for the sintering of compositions of β-Si_3N_4 solid solution (βss) [18–20].

(ii) βss materials with a low Al^{3+} content can only be totally densified by the presence of excess oxygen which then yields an amorphous phase upon cooling [19–22].

(iii) Impurities can be the cause of glass formation [6, 7, 23–26].

The present paper investigates materials with a composition of β 11 (11 eq% Al^{3+}). This composition was chosen to avoid crystallization of Si_2N_2O and the mullite-type $X_1(Si_{12}Al_{18}N_8O_{39})$ phase [17], in order to obtain a two-phase material of βss and amorphous phase only.

For the comparison of material properties of Si_3N_4 ceramics of different composition and processing the microstructure is an essential parameter. In connection with the properties it allows a complete characterization of these complex materials.

This investigation is aimed at testing:

(1) The possibility of quantitative microstructural analysis in such materials.

(2) The amount and distribution of the amorphous phase.

(3) The influence the amorphous phase has on the microstructure formation in regard to: (a) porosity, total and relative density; (b) grain size and shape.

2. Experimental procedure

2.1. Sample preparation

The starting compounds used for these investigations are listed in Table I. The powders were weighed, milled and mixed in an attritor mill with Al_2O_3 balls for 12 h in n-hexane. The wear of the balls was taken into account for the final composition. The mixtures were then dried, sieved and hot-pressed in BN coated graphite dies under a pressure of 35 MPa at 2043 K for 45 or 60 min. After firing, the surface layer was ground off and the density was measured by the Archimedes

0022–2461/82/061571–08$03.46/0

TABLE I Specification of the starting powders

Type	Source	Chemical composition (wt%)					Specific surface ($m^2\ g^{-1}$)
α–Si_3N_4	Starck, Berlin	37.1 N	0.01 Fe	0.06 Al	0.001 K	0.4 C	
	HCST 3510 Qu. 2	60.1 Si_{total}	0.03 Ca	0.002 Ti	0.0005 Li	2.0 O	8.8
		0.5 Si_{free}	0.003 Mg	0.003 Na	0.01 W		
AlN	Starck, Berlin HCST 530	31.85 N	65.03 Al	3.12 O			–
Al_2O_3	ALCOA A 16	52.9 Al	47.0 O	0.1 MgO			8.7

method. The phase analyses of the crystalline phases were performed using a Philips goniometer with CuKα radiation and with a LiF single crystal monochromator. The specimen composition, fabrication conditions and the results of the density measurements and phase analysis are listed in Table II. Fig. 1 shows the SiAlON system [17] with the five compositions A to E prepared.

2.2. Transmission electron microscopy

2.2.1. Specimen preparation

Discs of about 3 mm diameter were drilled out by ultrasonic cutting from the hot-pressed pellets. The discs were ground down to a thickness of about 50 μm and subsequently ion-beam thinned by argon. Finally a thin layer of carbon or aluminium was evaporated on to the sample to inhibit electric charging during the observations in the TEM.

2.2.2. Evaluation of TEM micrographs

The TEM micrographs were taken in a JEM 200 A microscope with an accelerating voltage of 200 kV. Several overview pictures were taken with a high voltage microscope operated at 1 MV. From the TEM micrographs the minimal prism diameter of the βss grains together with a shape parameter, describing the preferential shape of the βss grains, were determined. Furthermore, the volume-fraction of the amorphous phase was determined. The minimal prism diameter was evaluated by directly measuring the minimal length between two opposite $\{10\bar{1}0\}$ prismatic planes which are projected into the optical plane. For the determination of the shape parameter the cross-sectional area of the grains in the optical plane was measured together with their circumference by semi-automatic image analysis. Point and area analyses were used to estimate the content of amorphous phase in the triple-points where three or more grains join. For a first estimation of the thickness of the grain boundary layer, direct measurements can be used. However, these measurements include two possibilities for errors: First, the absorption of the carbon coating may yield a too small value for the grain boundary width. Secondly, surface cavity formation can yield too large values by image broadening of the amorphous phase. These surface cavities form at the grain boundaries upon ion thinning because of the uneven hardness of crystalline and amorphous phases. Another more accurate method is described by Clarke [9] and Krivanek *et al.* (27) who use microdensitometry: from the micrograph an intensity profile is taken across the grain boundary and across an adjacent triple-point. This was done 20 times for each specimen with consistently good results.

3. Experimental results

3.1. Phase analysis and density measurements

The X-ray phase analysis shows βss as the predominant phase in all samples. X_1 and Si could be detected in minimal amounts just above the detectability limit. The TEM investigations show the few X_1 grains reprecipitated as long needles from the

TABLE II Composition, hot-pressing conditions, phase composition and density

Sample	Si (eq %)	Al (eq %)	O (eq %)	N (eq %)	T(K)	t(min)	d(g cm^{-3})	Phases (X-ray)
A	89.4	10.6	7.5	92.5	2050	60	2.67	βss, (Si)
B	89.4	10.6	9.2	90.8	2040	45	3.150	βss, (Si)
C	89.4	10.6	10.9	89.1	2040	45	3.136	βss, (Si)
D	89.4	10.6	12.6	87.4	2040	45	3.116	βss, (X_1), (Si)
E	89.4	10.6	14.0	86.0	2040	45	3.103	βss, (X_1), (Si)

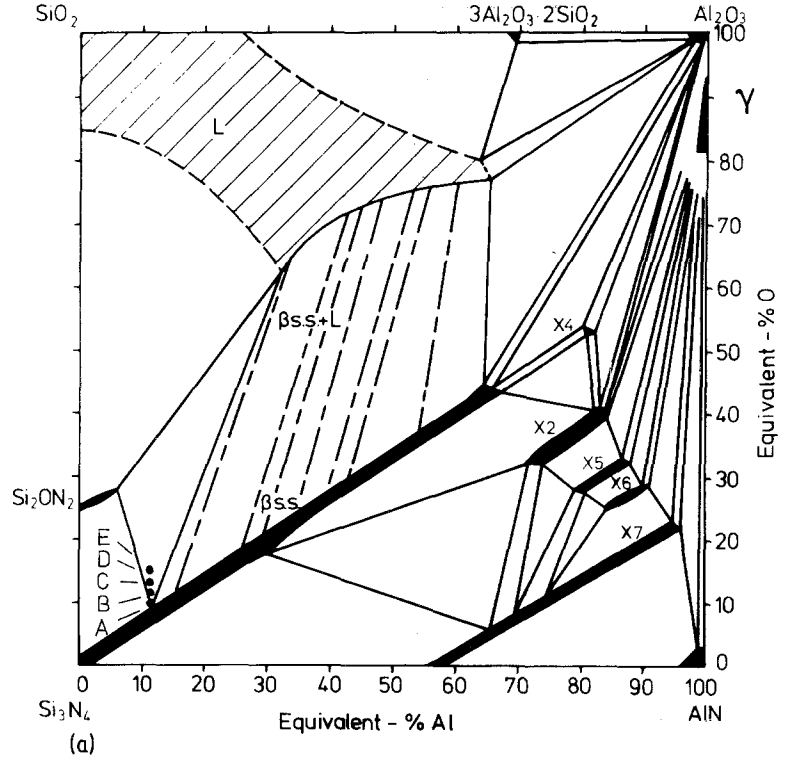

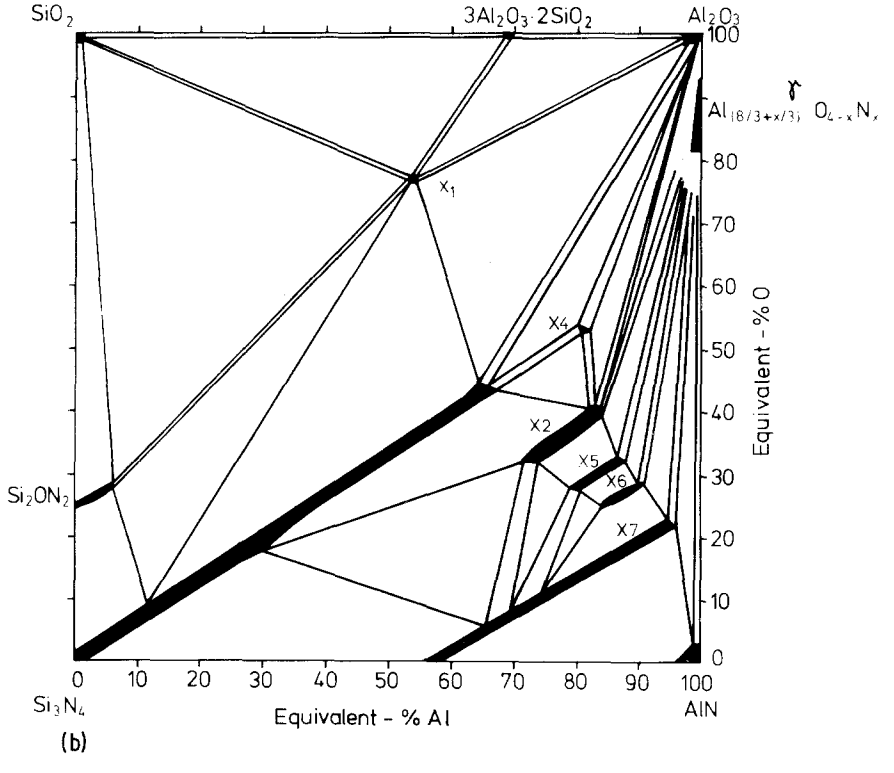

Figure 1 The SiAlON system after Naik *et al.* [17]: (a) at 2023 K with the compositions of the specimen prepared and (b) sub-solidus phase equilibria with X_1 (= $Si_{12}Al_{18}N_8O_{39}$) crystallized from the liquid phase L.

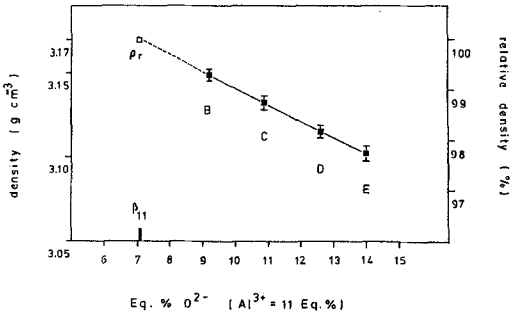

Figure 2 Densities measured by Archimedes method and density relative to the X-ray density of β 11, ρ_t is the theoretical density of β 11.

amorphous phase upon cooling. The amorphous phase was detected by TEM only. No detectable porosity was found by light microscopy and SEM in all samples except in those of the composition A, which revealed about 14% porosity.

The densities shown in Fig. 2 exhibit a nearly linear decrease with increasing oxygen content. These results were used in a first approximation for the estimation of the volume-fraction of the amorphous phase. This estimation can be made, if the density of the amorphous phase is known as well as the overall density and the βss density and if no porosity is found which is the case in the samples of the Compositions B to E. For the X-ray density of βss the lattice parameters measured by Gauckler *et al.* [28] were used, which correlate the lattice parameters to the Al^{3+} concentration. The density of the amorphous phase has to be estimated by the numerous results for compositions and densities of glass found in the literature [6, 7, 27, 29–31] and listed in Table III. Pure SiO_2 glasses have a density of 2.3 g cm^{-3}; MgO and CaO additions can raise it to 2.68 g cm^{-3} and higher. Nitrogen should also increase the density of such glasses [31]. From these results a constant glass density of 2.5 g cm^{-3} was estimated. This is of course only an approximation because the amount of amorphous phase has an influence on the impurity concentration, which decreases with increasing volume-fraction and thus lowers the density. However this shift in the density should be small and thus the constant value of 2.5 g cm^{-3} is justified for a first approximation. These results are discussed and compared to the evaluation of the TEM micrographs later on.

3.2. TEM microstructure evaluation

Several examples of TEM micrographs are shown in Figs 3 and 4. They allow a determination of the influence that the amount of the amorphous phase has on the preferred grain shape, prism diameter, grain boundary geometry and dislocation density in the βss crystals near the grain boundaries.

3.2.1. Grain shape

In the presence of the amorphous phase, the βss crystals generally show a more prismatic morphology. To describe this preferential shape a shape parameter F_1, generally used in stereology, is introduced

$$F_1 = \frac{4\Pi A}{U^2}, \qquad (1)$$

where A is the cross-sectional area of one grain in the optical plane determined by area analysis with the MOP (semi-automatic image analyser) and U is the circumference of this grain. F_1 represents the deviation from an isometric crystal growth, projected and measured in the optical plane. The standard deviation of F_1 indicates the difference in shape measurements and their consequences for the three-dimensional orientations. The shape parameter is shown in Fig. 5 together with the standard deviation and correlation to the oxygen content. For the βss crystals F_1 represents the elongation along the c-axis. In the presence of sufficient amounts of liquid, the ⟨0001⟩ direction is the preferred growth direction except for

TABLE III Densities of various glass compositions from literature

Reference	Composition in mole numbers					
	CaO	MgO	Al_2O_3	SiO_2	Si_3N_4	d (g cm^{-3})
[22]	0.4	0.75	–	2	–	2.54 calculated
[29]	0.15	0.64	0.22	2	–	2.45 calculated
[29]	0.076	0.42	0.22	2	–	2.41 calculated
[29]	–	2	2	5	–	2.36 calculated
[26]	1	1	–	2	–	2.68 calculated
[30]	–	4	–	7	0.5	2.58 measured
[6]	–	0.14	0.08	3	–	2.28 calculated

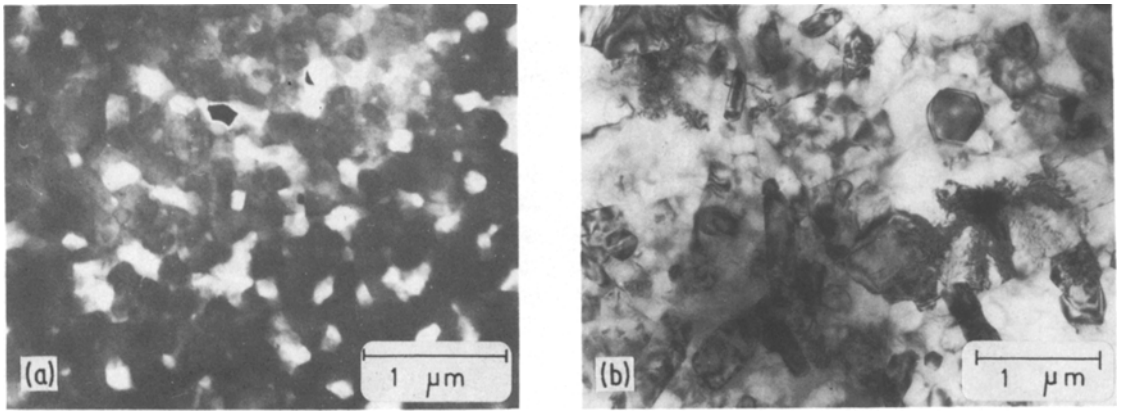

Figure 3 TEM bright-field micrographs (a) Composition A revealing 14% porosity, (b) Composition E with prismatic βss crystals.

Sample A, where more isometric-shaped cyrstals are found.

3.2.2. Prism diameter

The determination of the minimal prism diameter avoids the influence of the grain orientation relative to the optical plane. Fig. 6 shows that this average minimal prism diameter is hardly affected by the amount of oxygen present. However, from the grain shape parameter, the conclusion can be drawn that the needle length in the ⟨0001⟩ direction increases with increasing oxygen content. However, absolute values of the length cannot be estimated by this method.

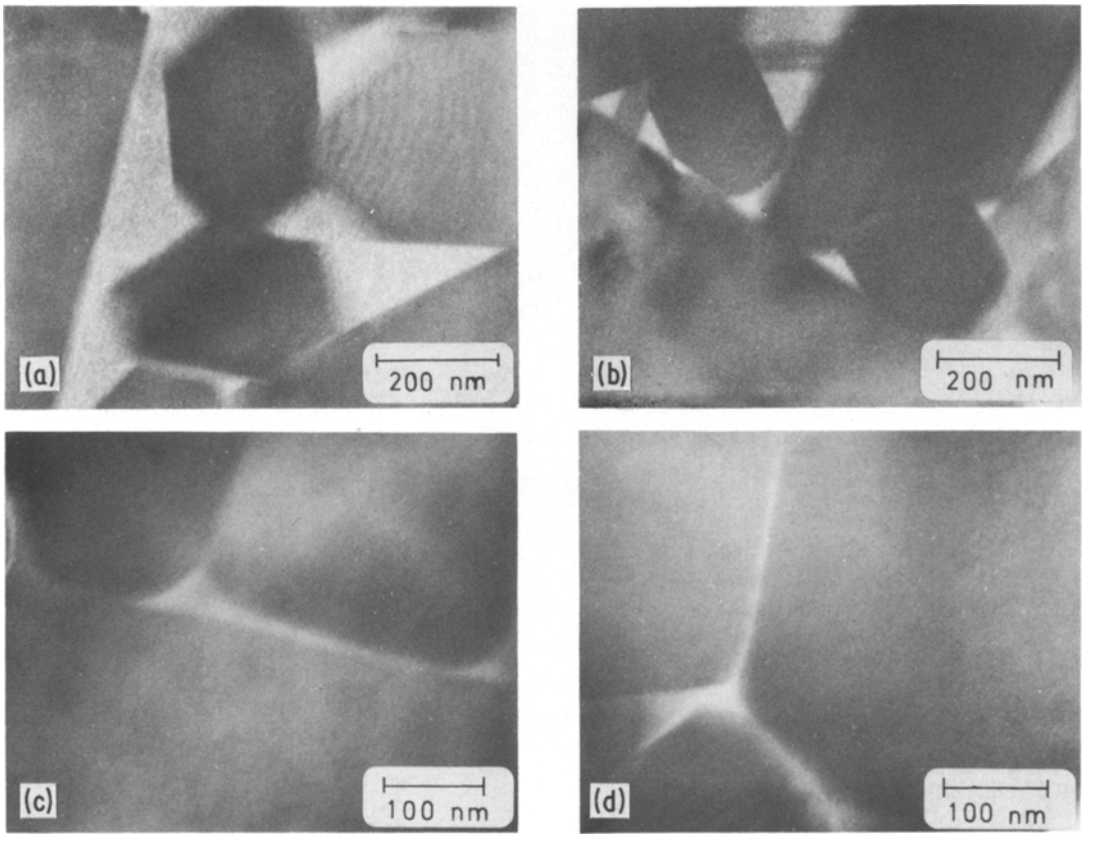

Figure 4 TEM dark-field micrographs: (a) and (b) Composition E, showing amorphous phase content in triple-points. (c) and (d) Compositions B and E, showing amorphous grain boundary phases between βss crystals.

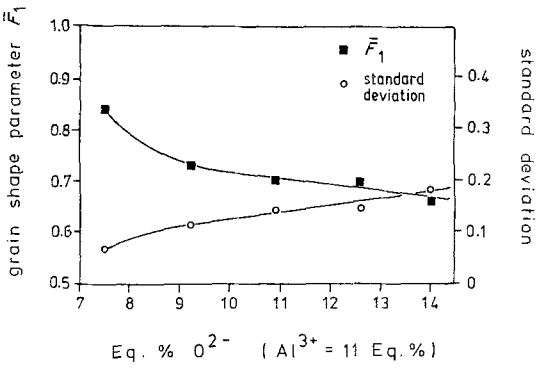

Figure 5 Grain shape parameter $F_1 = (4\pi A)/U^2$ and the standard deviation of F_1.

3.2.3. Grain boundary geometry

As shown in Fig. 4a to d, grain boundaries containing an amorphous phase are to a large extent planar without significant curvature except in the triple-points and without influence of the amount of the glassy phase. Materials of composition A show different results with many bent grain boundaries and a higher dislocation density at some grain boundaries. An example of this phenomenon is shown in Fig. 7. The bent lines and the occurrence of tension contrast, both indicate that there are dislocations and not moiré patterns. Several thickness contrasts can be seen parallel to the grain boundaries.

3.3. Determination of the volume-fraction of the amorphous phase by TEM methods

In order to determine the thickness and content of the grain boundary phase, two different TEM methods can be chosen [9, 27]:

3.3.1. Direct lattice imaging technique

This method yields the most accurate results [32–35] but requires much experimental effort and only reveals small regions of the specimens. Thus it can hardly be used in order to obtain statistical results.

3.3.2. Dark-field imaging

This method is less accurate because the grain boundary does not form a sharp contrast for direct measurements. More accurate results can be estimated by microdensitometry. The actual layer thickness was estimated in analogy to [9, 27] and calculated from the intensities by the formula

$$\Delta x \approx \frac{\int J(x_{gb}) \cdot dx_{gb}}{\bar{J}_{tr}}, \qquad (2)$$

where Δx is the grain boundary thickness, $J(x_{gb})$ is the intensity across the grain boundary, x_{gb} is the place at which the intensity $J(x_{gb})$ is measured and $\bar{J}_{tr}$ is the intensity at the adjacent triple-point. The results obtained by this method (Fig. 8) reveal that the amount of amorphous phase only slightly influences the layer width. In order to see if the amorphous carbon coating influences the apparent grain boundary width-one sample was coated with aluminium. Aluminium yields a crystalline surface coating and thus produces sharp diffraction patterns: the selected-area aperture only samples the actual grain boundary material. Under these conditions a comparison of the carbon and aluminium coated samples yielded values within the error bars. This shows that the carbon coating has no influence on the width as measured by microdensitometry.

4. Discussion

In order to estimate with this knowledge the volume-fraction of the glassy phase present in the grain boundaries, V_{gb}, the grain boundary surface area per unit volume has to be known. This volume can be estimated [36] by

$$A_{gb} = \frac{2N}{L_t}; \qquad (3)$$

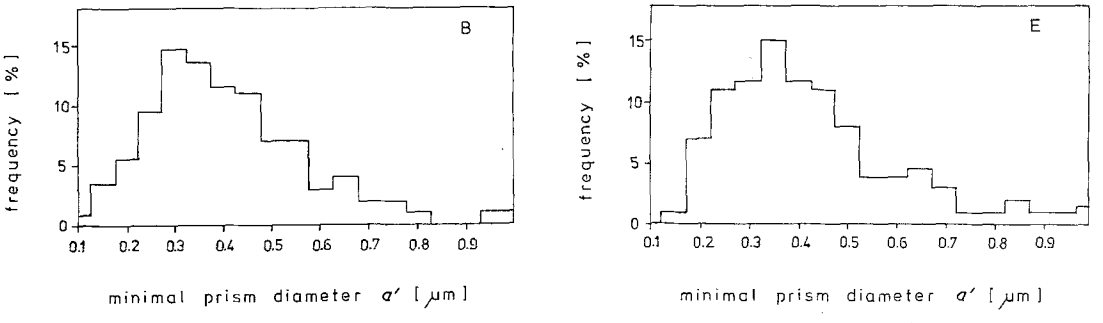

Figure 6 Minimal average grain prism diameter a', measured at samples of the Composition B and E.

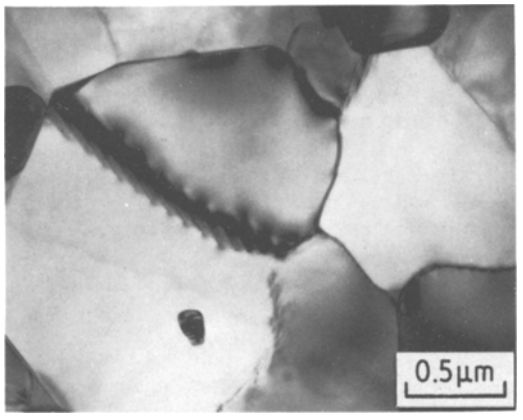

Figure 7 Material of Composition A with bent grain boundaries and significant dislocation density near grain boundaries.

hence,

$$V_{gb} = \frac{2N\,\Delta x}{L_t}, \qquad .(4)$$

where A_{gb} is the grain boundary area per unit volume, Δx is the grain boundary width (by TEM dark-field), N is the number of grains (by TEM bright-field) and L_t is the length analysed (by TEM bright-field), under the assumption of a constant grain boundary layer thickness and the presence of such a phase in between all grain boundaries. The first assumption neglects possible anistropy effects [33] but according to the present TEM investigations it should apply with good approximation. The latter neglects the various types of grain boundaries, where such a phase cannot be observed [34]. Therefore, this estimation yields the maximum possible value shown in Fig. 9 together with the volume-fraction in the triple-points. It shows that as soon as the amorphous phase has wetted all grain boundaries the

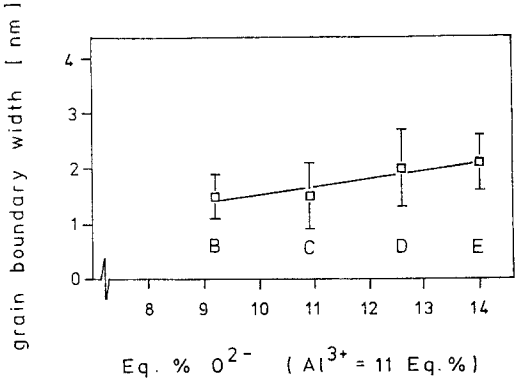

Figure 8 Thickness of the amorphous grain boundary layer.

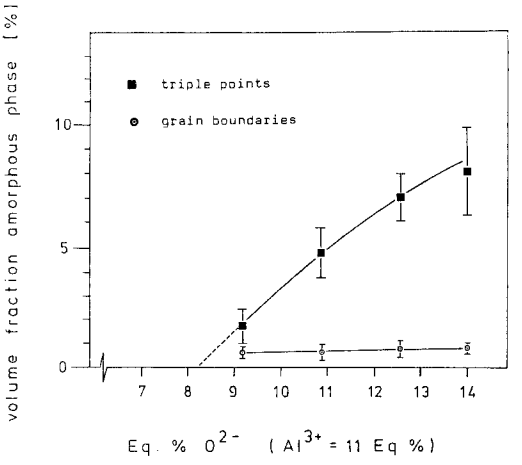

Figure 9 Volume-fraction amorphous phase in triple-points and grain boundaries (% of total volume).

surplus gathers in the triple-points. In Fig. 10 the estimation of the total content of amorphous phases estimated by TEM (triple-points + grain boundaries) is compared to those values obtained by density measurements and an estimation by the lever rule from the phase diagram of the SiAlON system. This estimation using the lever rule was done by assuming:

The amount of liquid is found if the composition of the nitrogen rich liquid shown in Fig. 1 [17] is used. The Si^{4+}: Al^{3+} ratio is assumed to be constant in the overall and liquid compositions. However, the range of the values obtained by these three estimations is comparatively small and this shows the possibility of quantitative estimation of finely distributed amorphous phases by TEM methods.

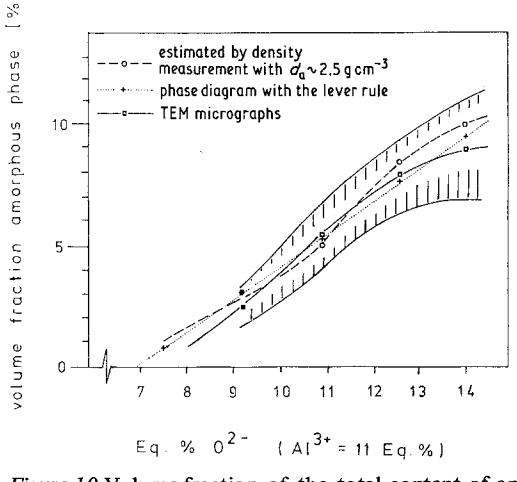

Figure 10 Volume-fraction of the total content of amorphous phase estimated by TEM, density and lever rule (⊥⊥⊥⊥ error bars of TEM evaluation).

Future measurements will be aimed at correlating these observations to high temperature strength and creep.

5. Conclusions

In this investigation the possibility of a quantitative microstructure analysis in Si_3N_4 ceramics has been tested. For this test a β solid solution material (βss) with 11 eq% Al^{3+} and varied oxygen/nitrogen ratio has been examined. The results show that such an analysis is possible within certain limits, set by the necessary use of transmission electron microscopy (TEM). For the βss material investigated, the results show the influence of the amorphous phase:

(1) Increasing amounts of amorphous phase increase the preferential orientation leading to a more fibrous prismatic grain morphology.

(2) Parallel to this behaviour goes an increase of the grain size along the *c*-axis while the prism diameter stays nearly constant. Without the presence of any amorphous phase the grain morphology alters completely to more irregular shapes.

(3) The grain boundary width is rather insensitive to the content of the amorphous phase.

(4) When all grain boundaries are wetted with a grain boundary phase, all the surplus of this phase is contained in the triple-points.

(5) The TEM estimations yield a value of the volume fraction in good agreement with direct density measurements and estimations from the phase diagram by the level rule and thus outline the possibility of such a procedure for finely distributed grain boundary films.

Acknowledgements

The authors thank Dr M. Rühle and Dr M. Kirn for their advice and helpful discussions. Financial support by the Bundesministerium für Forschung und Technologie (BMFT) is gratefully acknowledged.

References

1. A. G. EVANS and J. V. SHARP, *J. Mater. Sci.* 6 (1971) 1292.
2. R. KOSSOWSKY, *ibid.* 8 (1973) 1603.
3. P. DREW and M. H. LEWIS, *ibid.* 9 (1974) 261.
4. *Idem, ibid.* 9 (1974) 1833.
5. M. RÜHLE, C. SPRINGER, L. J. GAUCKLER and M. WILKENS, Proceedings of the Fifth Conference on High Voltage Electron Microscopy, Kyoto, August/September 1977, edited by T. Imura and H. Hashimoto (1977) p. 641.
6. L. K. V. LOU, T. E. MITCHELL and A. H. HEUER, *J. Amer. Ceram. Soc.* 61 (1978) 392.
7. *Idem, ibid.* 61 (1978) 462.
8. P. M. JOHNSON and A. HENDRY, *J. Mater. Sci.* 14 (1979) 2439.
9. D. R. CLARKE, *Ultramicroscopy* 4 (1979) 33.
10. R. KOSSOWSKY, D. G. MILLER and E. S. DIAZ, *J. Mater. Sci.* 10 (1975 983.
11. M. S. SMELTZER, *Bull. Amer. Ceram. Soc.* 56 (1977) 418.
12. F. F. LANGE, B. I. DAVIS and D. R. CLARKE, *J. Mater. Sci.* 15 (1980) 611.
13. B. S. B. KARUNARATNE and M. H. LEWIS, *ibid.* 15 (1980) 449.
14. L. J. BOWEN, R. J. WESTON, T. G. CARRUTHERS and R. J. BROOK, *ibid.* 13 (1978) 341.
15. L. J. BOWEN, T. G. CARRUTHERS and R. J. BROOK, *J. Amer. Ceram. Soc.* 61 (1978) 335.
16. L. J. GAUCKLER, H. L. LUKAS and G. PETZOW, *ibid.* 58 (1975) 346.
17. I. K. NAIK, L. J. GAUCKLER and T. Y. TIEN, *ibid.* 61 (1978) 332.
18. S. BOSKOVIC, L. J. GAUCKLER, G. PETZOW and T. Y. TIEN, *Powder Met. Int.* 9 (1977) 184.
19. *Idem, ibid.* 10 (1978) 184.
20. *Idem, ibid.* 11 (1979) 169.
21. M. KUWABARA, M. BENN and F. L. RILEY, *J. Mater. Sci.* 15 (1980) 1407.
22. R. E. LOEHMAN and D. J. ROWCLIFFE, *J. Amer. Ceram. Soc.* 63 (1980) 144.
23. B. D. POWELL and P. DREW, *J. Mater. Sci.* 9 (1974) 1867.
24. S. HOFMANN and L. J. GAUCKLER, *Powder Met. Int.* 6 (1974) 90.
25. D. W. RICHERSON, *Bull. Amer. Ceram. Soc.* 52 (1973) 560.
26. L. J. ISKOE, F. F. LANGE and E. S. DIAZ, *J. Mater. Sci.* 11 (1976) 908.
27. O. L. KRIVANEK, T. M. SHAW and G. THOMAS, *J. Amer. Ceram. Soc.* 62 (1979) 585.
28. L. J. GAUCKLER, J. WEISS, T. Y. TIEN and G. PETZOW, *J. Amer. Ceram. Soc.* 61 (1978) 397.
29. M. L. HUGGINS and K. H. SUN, *ibid.* 26 (1943) 4.
30. M. H. LEWIS, B. D. POWELL, P. DREW, R. J. LUMBY, B. NORTH and A. J. TAYLOR, *J. Mater. Sci.* 12 (1977) 61.
31. K. H. JACK, in "Nitrogen Ceramics", edited by F. L. Riley (Noordhoff, Leyden, 1977) pp. 257–62.
32. D. R. CLARKE and G. THOMAS, *J. Amer. Ceram. Soc.* 60 (1977) 491.
33. *Idem, ibid.* 61 (1978) 114.
34. M. KIRN, PhD thesis, University of Stuttgart, 1979.
35. H. SCHMID, PhD thesis, University of Stuttgart, 1980.
36. S. A. SALTYKOV, "A Stereological Method for Measuring the Specific Surface Area of Metallic Powders", (Springer-Verlag, Berlin, 1967) p. 63.

Received 9 March
and accepted 27 April 1981